Electronic Supplementary Material (ESI) for Physical Chemistry Chemical Physics.

Supporting Information

Insights from Ion Mobility – Mass Spectrometry, Infrared Spectroscopy, and Molecular Dynamics on Nicotinamide Adenine Dinucleotide Structural Dynamics: NAD^+ *vs* NADH

Juan Camilo Molano-Arevalo,[†] Walter Gonzalez,[†] Kevin Jeanne Dit Fouque,[†] Jaroslava Miksovska,[†,‡] Philippe Maitre,[*,§] and Francisco Fernandez-Lima,[*,†,‡]

[†] Department of Chemistry and Biochemistry, Florida International University, Miami, FL 33199, USA

[‡] Biomolecular Sciences Institute, Florida International University, Miami, FL 33199, USA

[§] Laboratoire de Chimie Physique, Université Paris Sud, UMR 8000 CNRS, 91405 Orsay Cedex, France

AUTHOR INFORMATION

Corresponding Author: fernandf@fiu.edu

Table of Contents

Figure S1. TIMS instrument scheme

Figures S2-S7. Lowest energy candidate structures proposed for the protonated NADH and NAD^+ IMS bands

Figure S8. Theoretical IR spectra of NADH and NAD^+

Figure S9. Labeled atoms present in the structure of NADH and NAD^+

Figure S10. Intramolecular interactions of NADH and NAD^+

Figure S11. Intramolecular interactions of NADH and NAD^+ sorted by the three main conformational families

Figure S12-S15. Lowest energy candidate structures proposed for the sodiated NADH and NAD^+ IMS bands

Figure S16. Intramolecular interactions of the sodiated species of NADH and NAD^+ sorted by the three main conformational families.

Table S1. Fluorescence decay parameters of NADH as a function of EtOH or MeOH content

Table S2. Experimental and theoretical CCS for the sodiated NAD^+ and NADH forms

Table S3. Experimental and theoretical CCS and experimental vibrational frequencies for the protonated NADH form

Table S4. Experimental and theoretical CCS and experimental vibrational frequencies for the protonated NAD^+ form

Table S5. Theoretical intramolecular interactions of NADH

Table S6. Theoretical intramolecular interactions of NAD^+

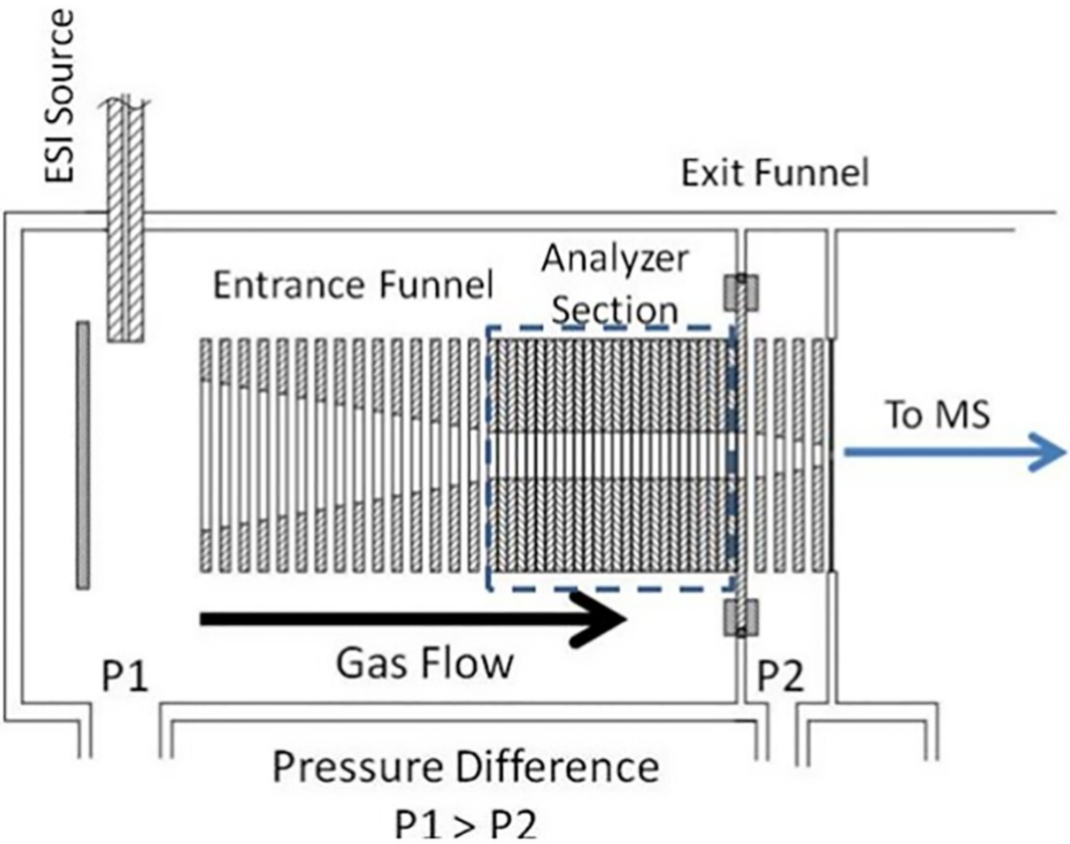

Figure S1. Scheme of the TIMS cell

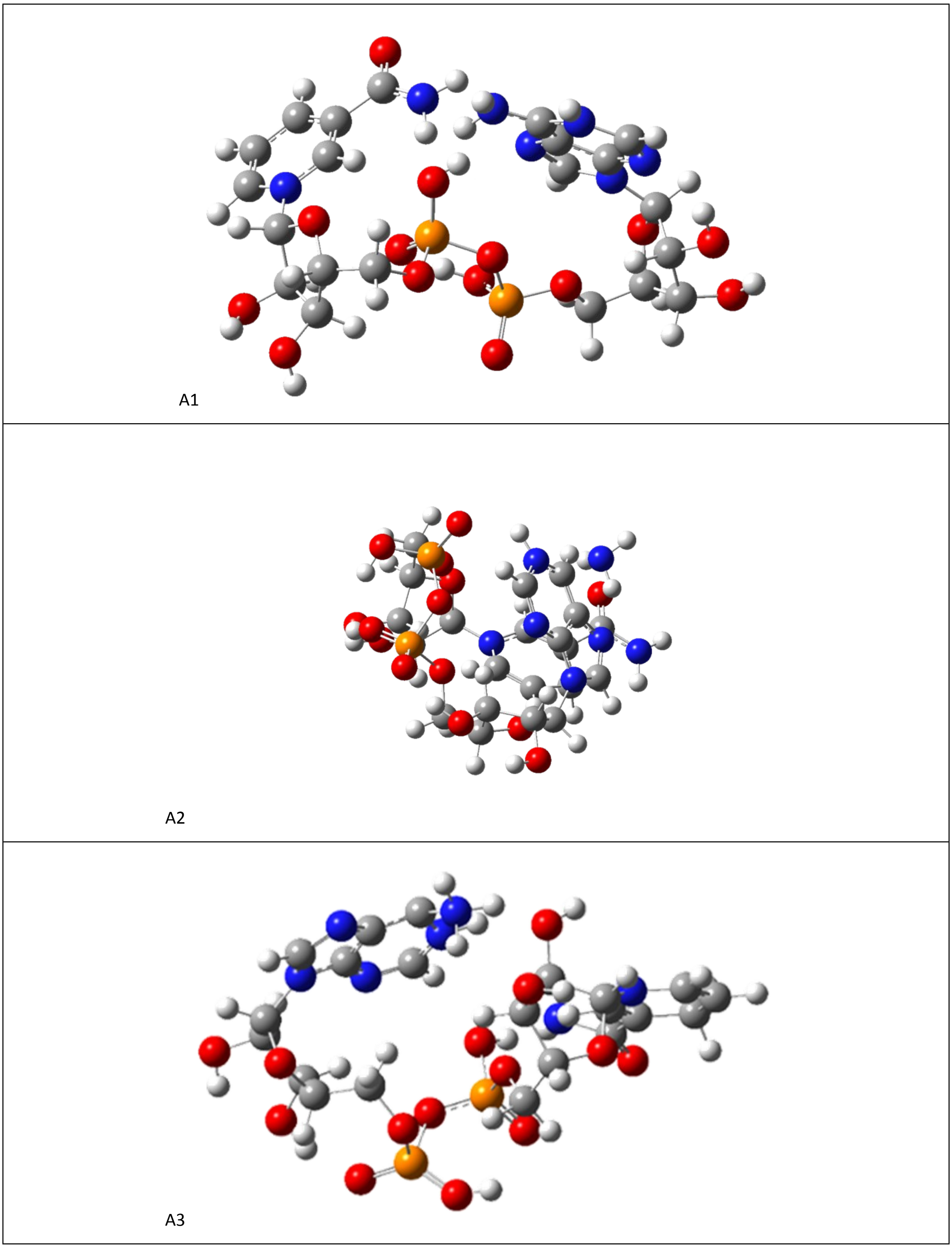

Figure S2. Lowest energy candidate structures proposed for NADH IMS band A obtained at DFT/B3LYP/6-31G*using Jaguar software.

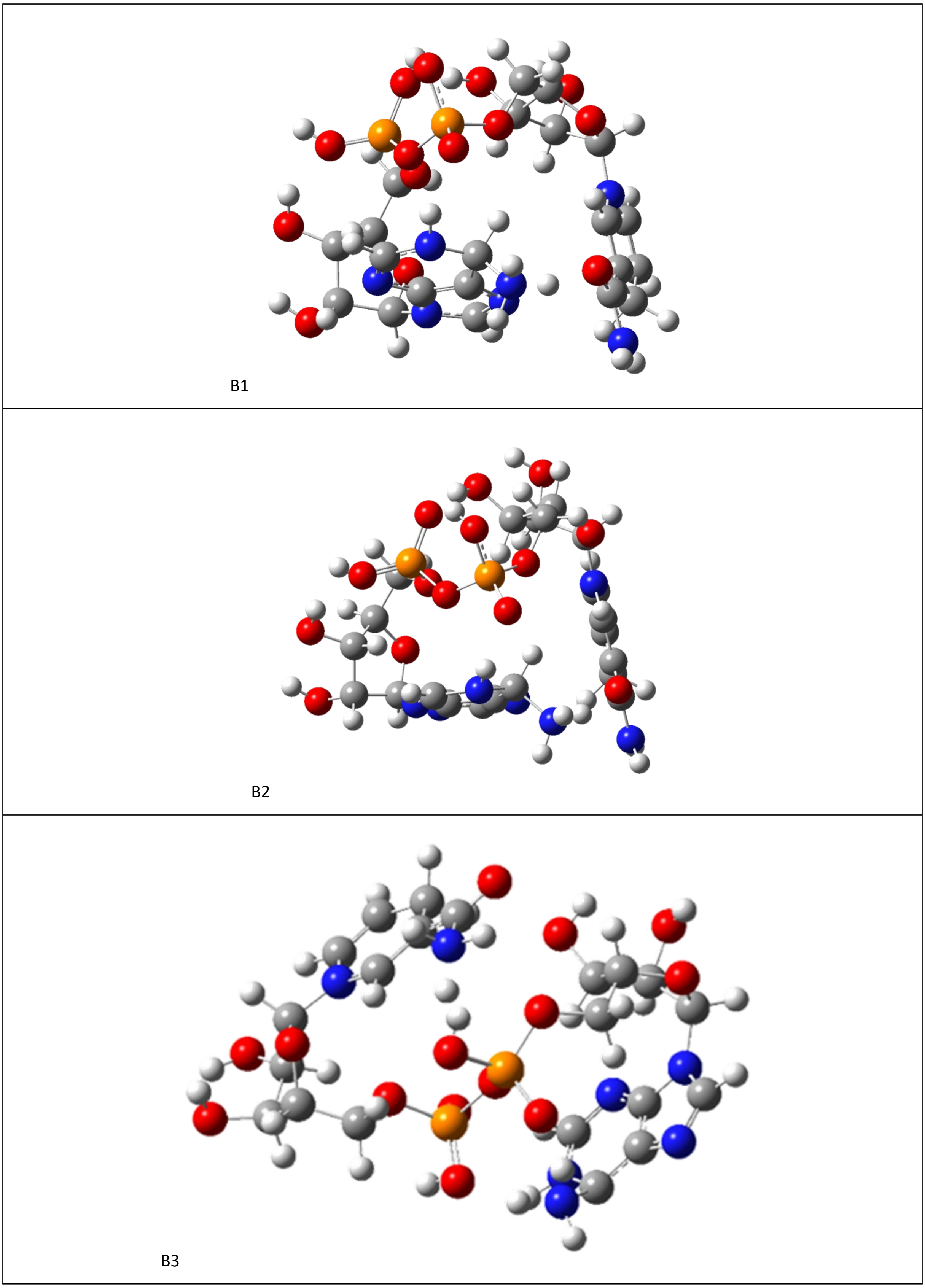

Figure S3. Lowest energy candidate structures proposed for NADH IMS band B obtained at DFT/B3LYP/6-31G*using Jaguar software.

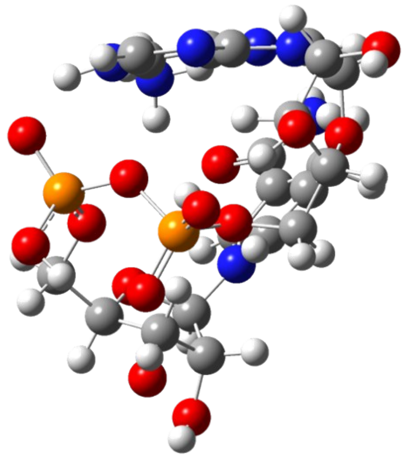

C1

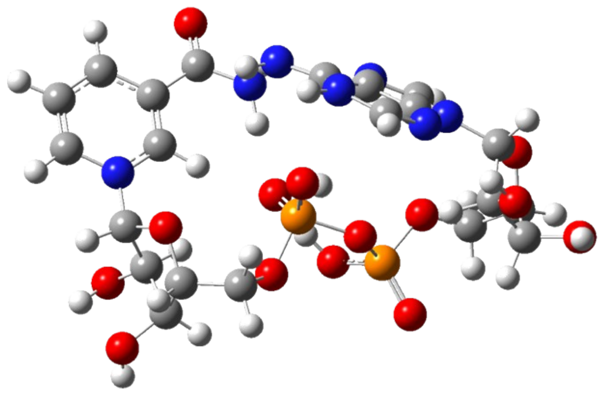

C2

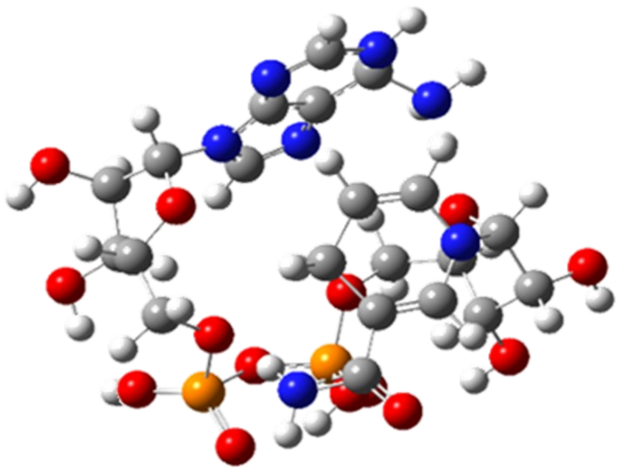

C3

Figure S4. Lowest energy candidate structures proposed for NADH IMS band C obtained at DFT/B3LYP/6-31G*using Jaguar software.

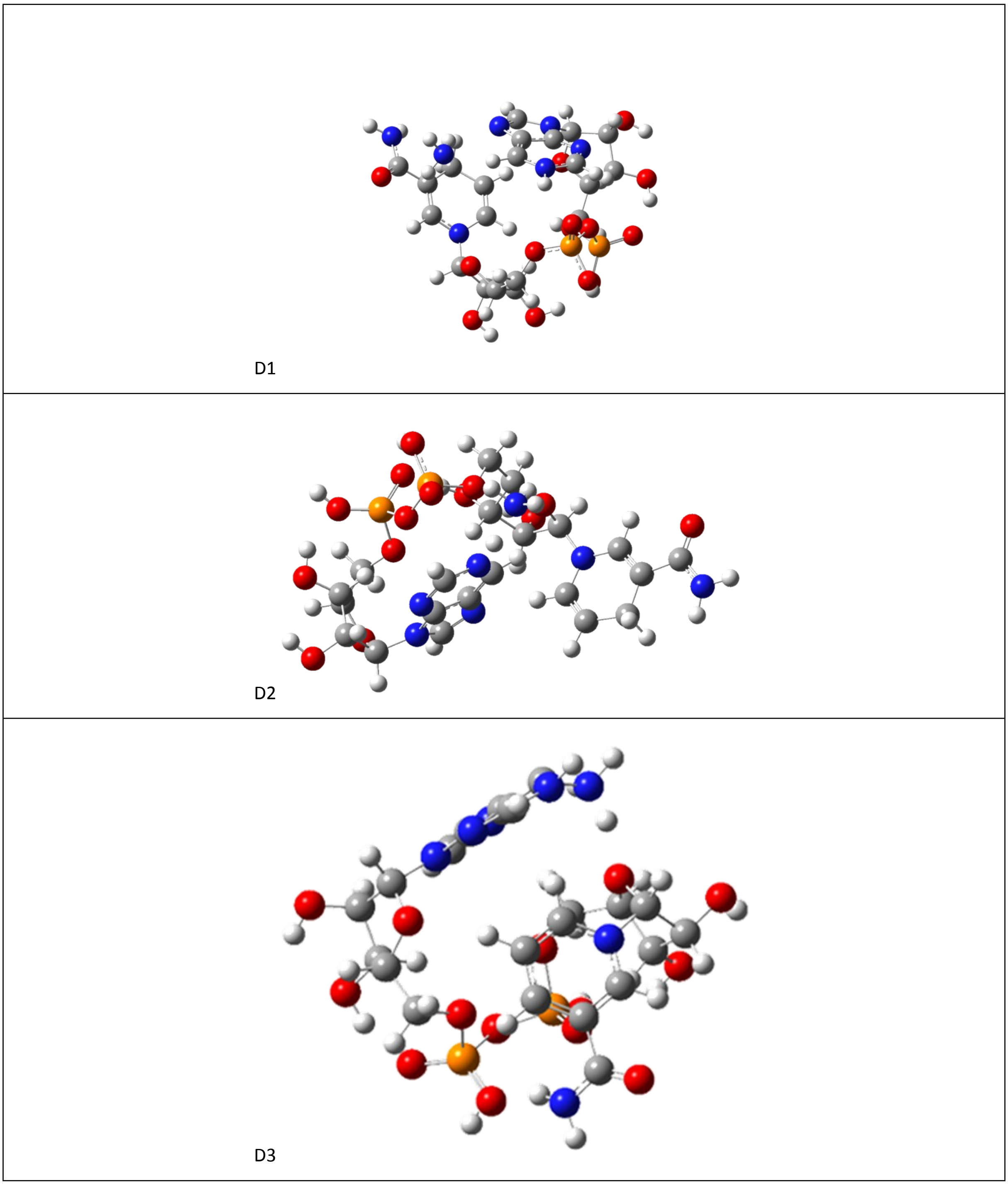

Figure S5. Lowest energy candidate structures proposed for NADH IMS band D obtained at DFT/B3LYP/6-31G*using Jaguar software.

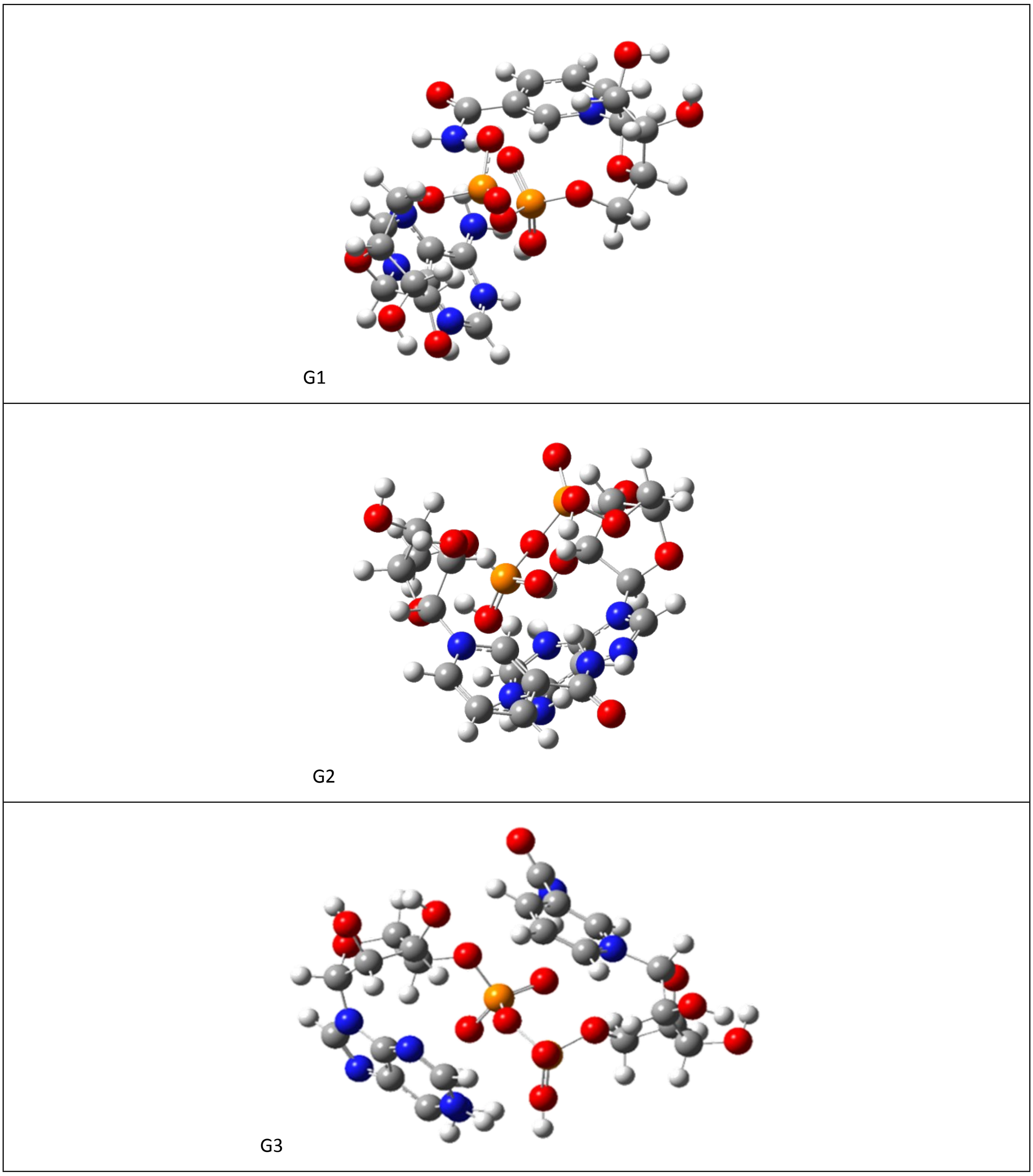

Figure S6. Lowest energy candidate structures proposed for NADH IMS band G obtained at DFT/B3LYP/6-31G*using Jaguar software.

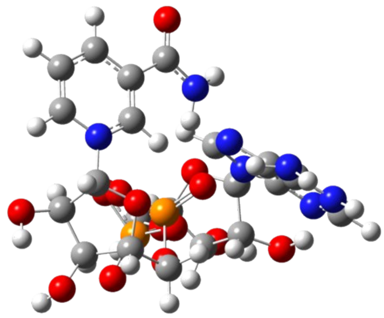

H1

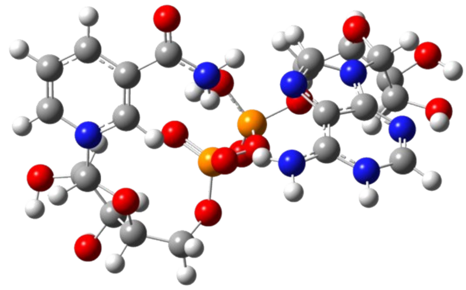

H2

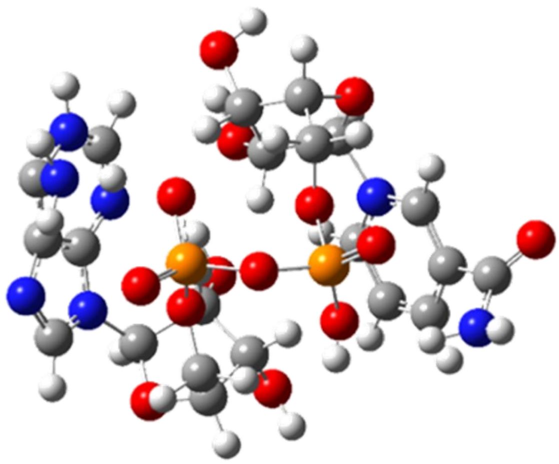

H3

Figure S7. Lowest energy candidate structures proposed for NADH IMS band H obtained at DFT/B3LYP/6-31G*using Jaguar software.

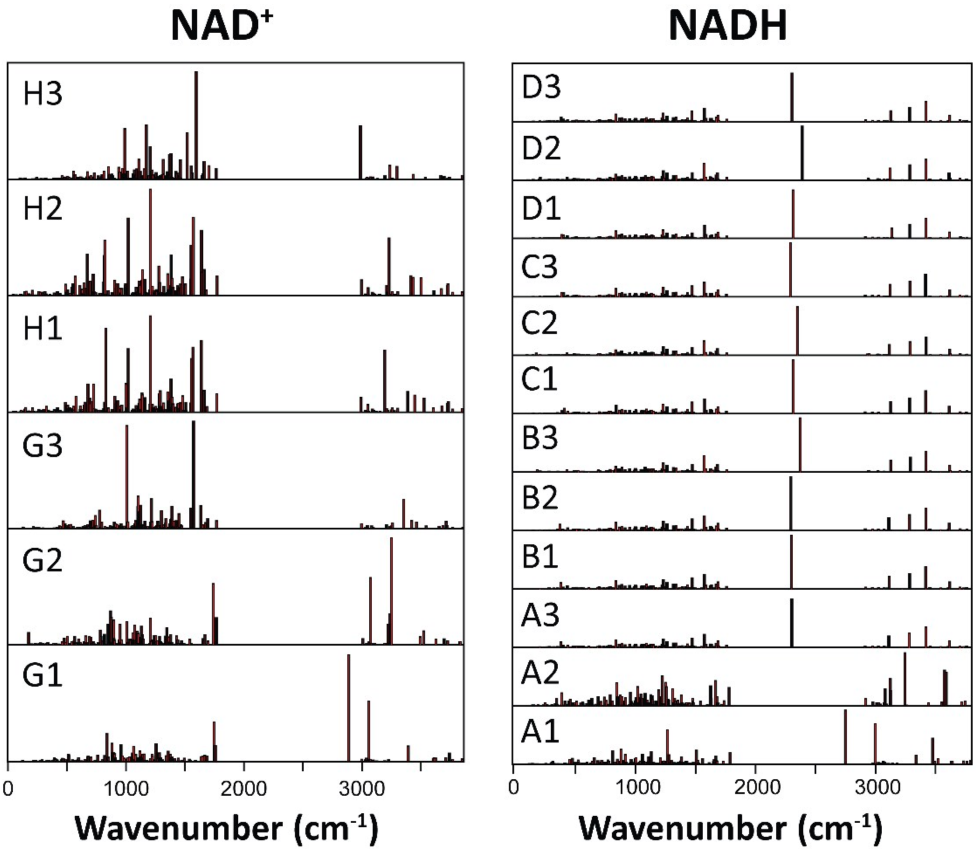

Figure S8. Theoretical IR spectra of NAD^+ and NADH obtained at DFT/B3LYP/6-31G* using Jaguar software.

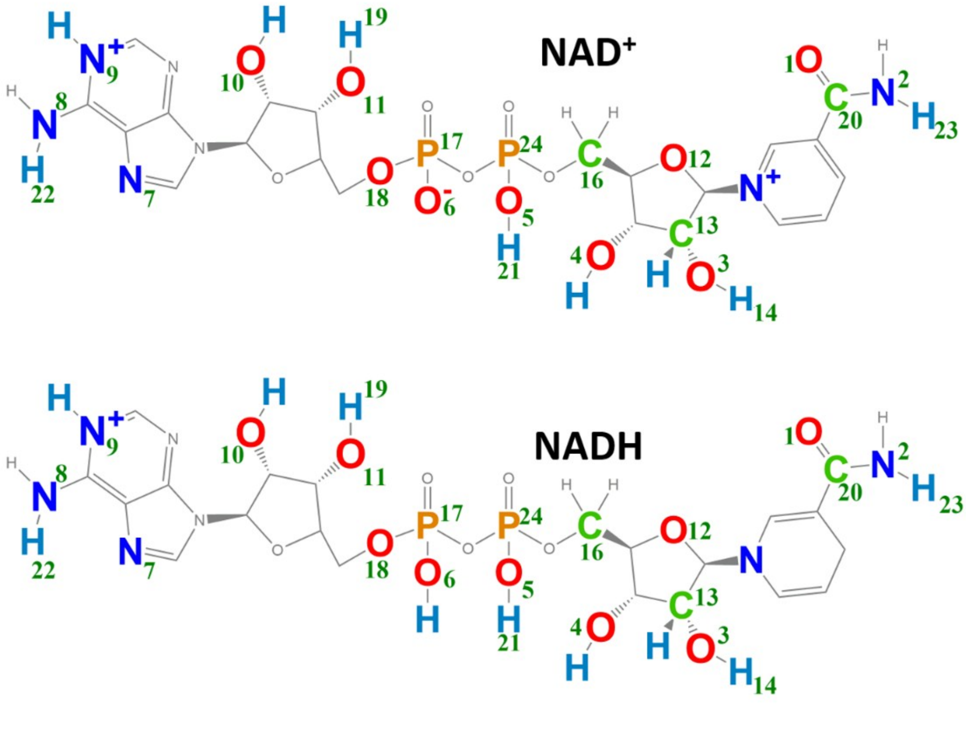

Figure S9. Labeled atoms present in the structure of NADH and NAD^+.

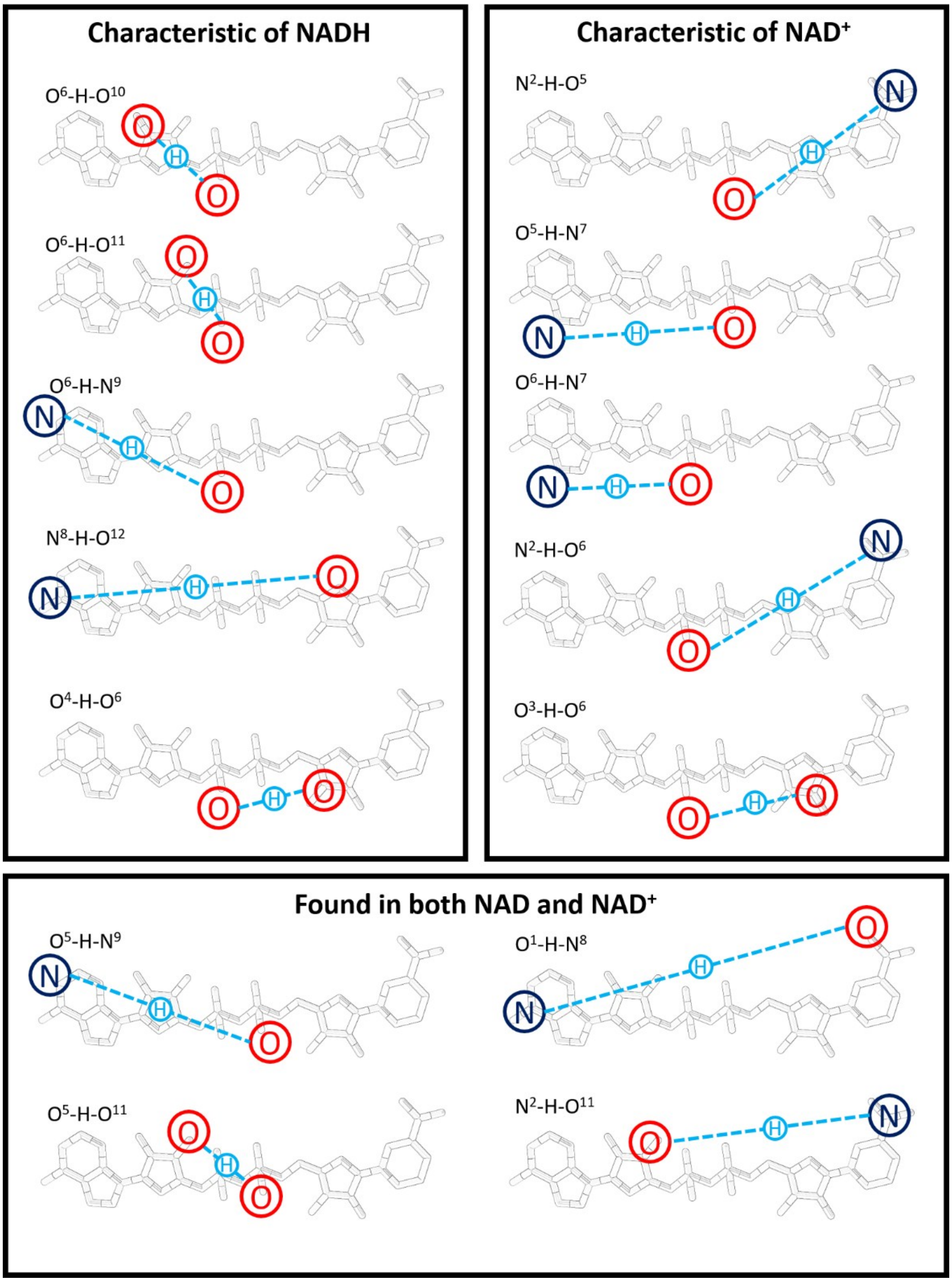

Figure S10. Intramolecular interactions of NADH and NAD^+.

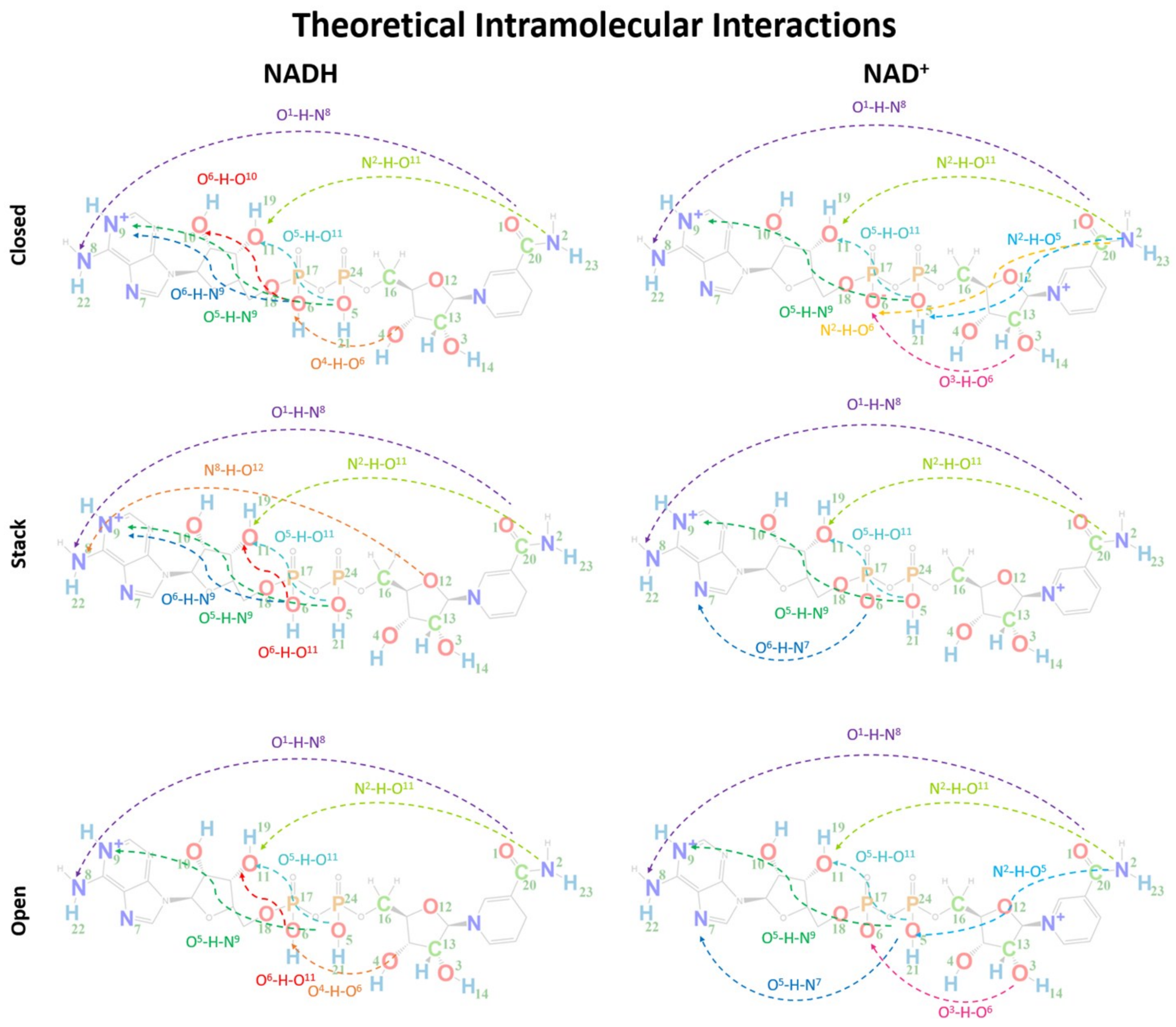

Figure S11. Intramolecular interactions of NADH and NAD^+ sorted by the three main conformational families.

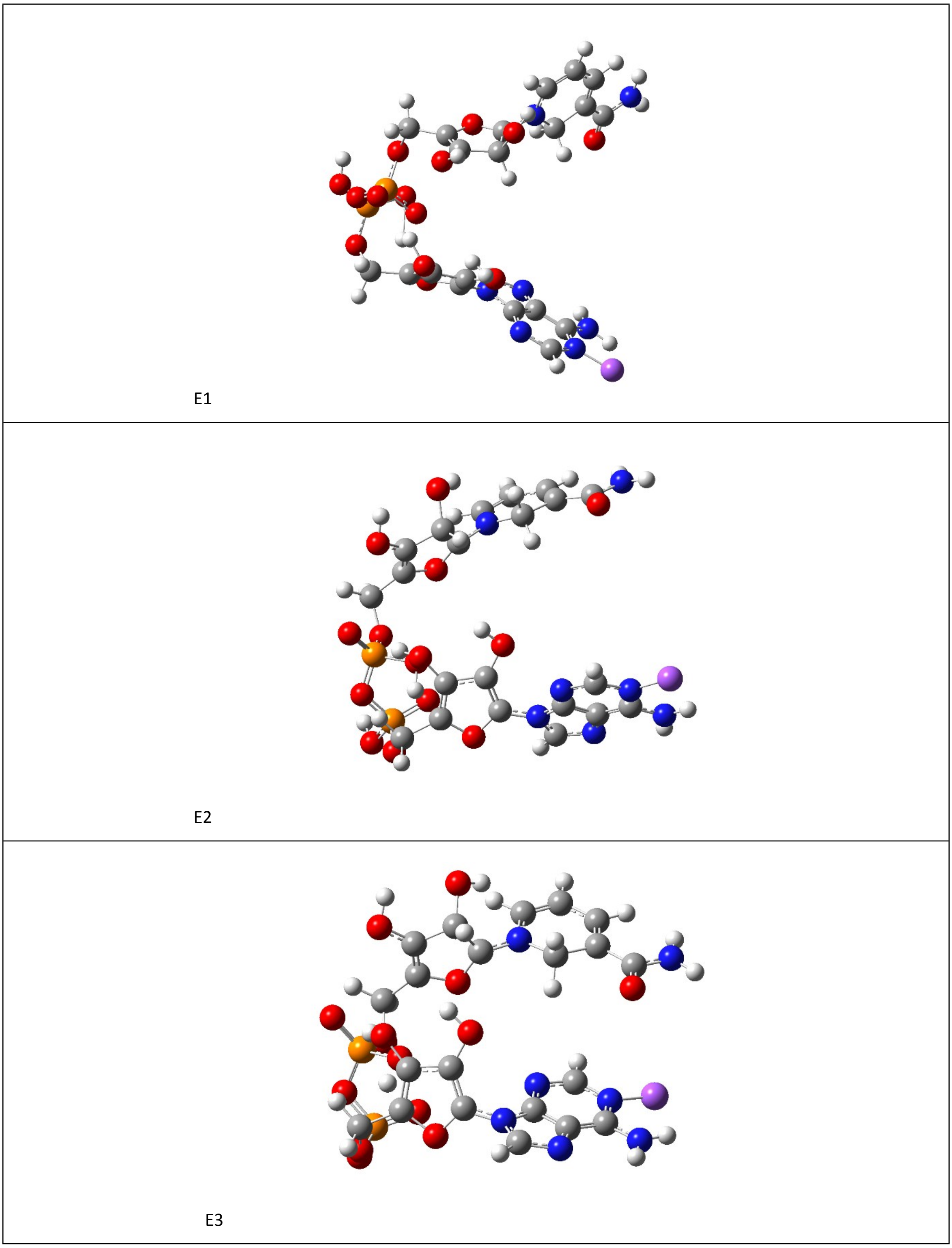

Figure S12. Lowest energy candidate structures proposed for the sodiated NADH IMS band E obtained at DFT/B3LYP/6-31G*using Jaguar software.

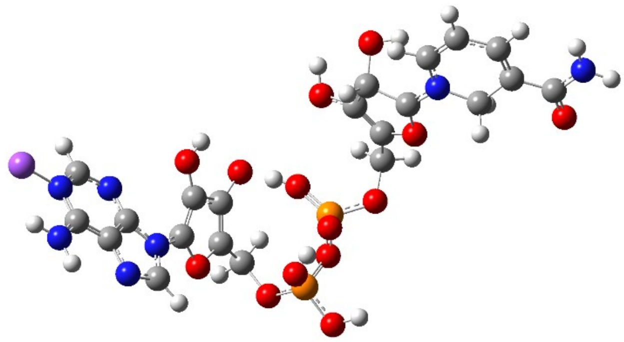

F1

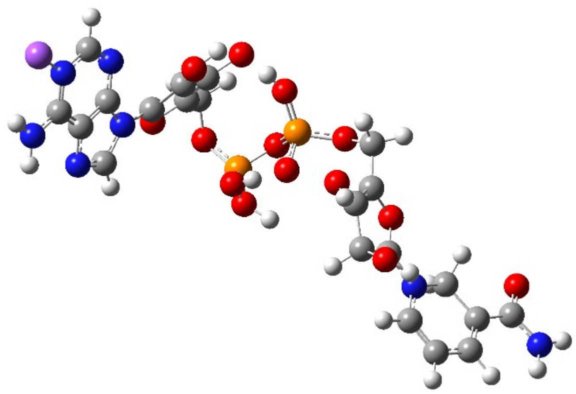

F2

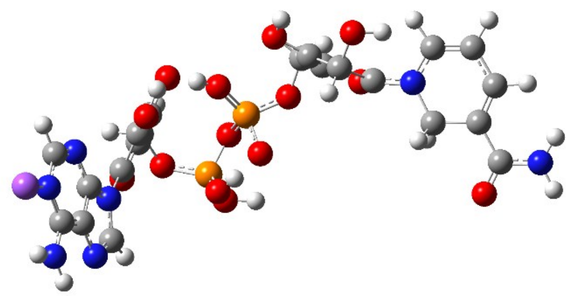

F3

Figure S13. Lowest energy candidate structures proposed for the sodiated NADH IMS band F obtained at DFT/B3LYP/6-31G*using Jaguar software.

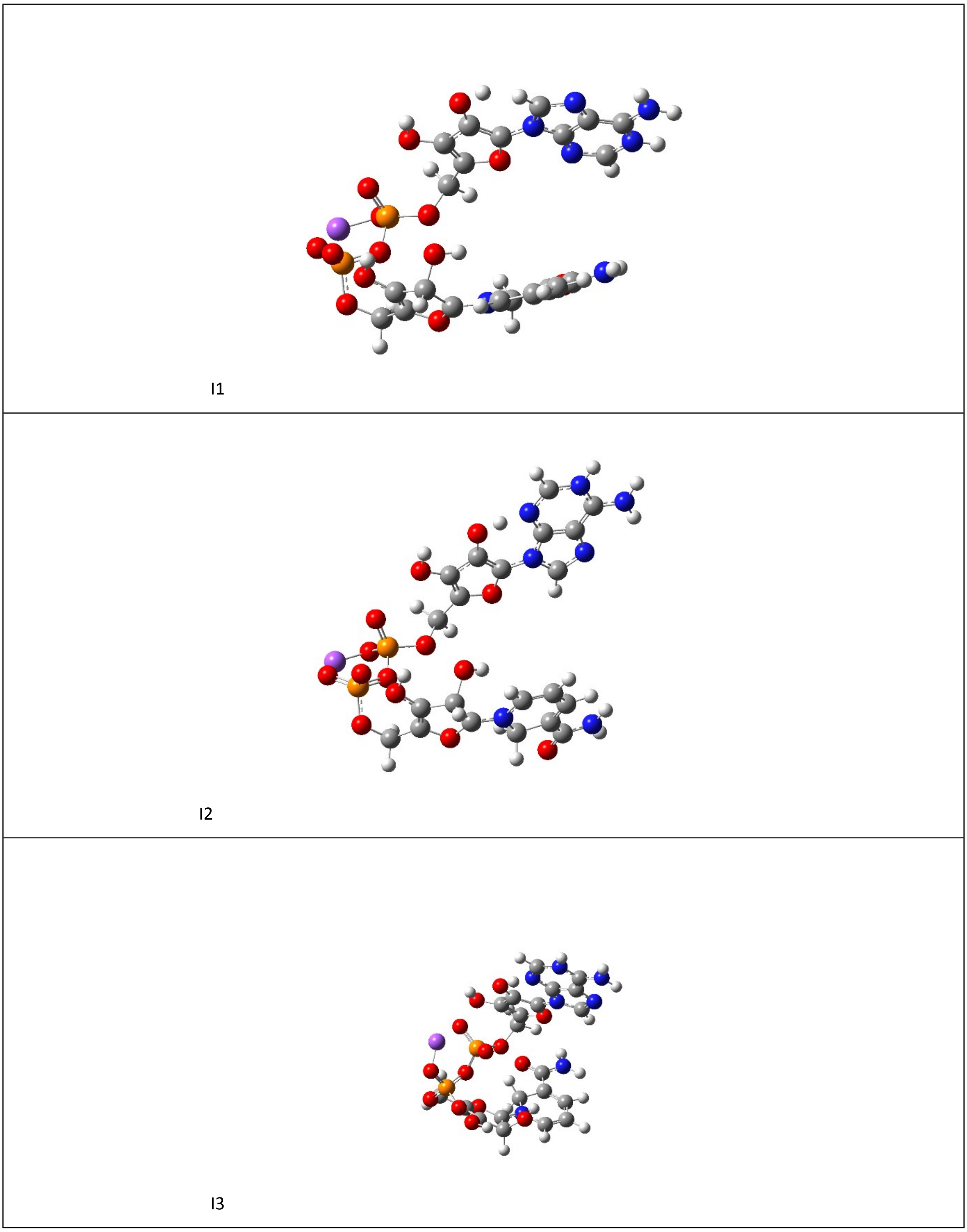

Figure S14. Lowest energy candidate structures proposed for the sodiated NAD^+ IMS band I obtained at DFT/B3LYP/6-31G*using Jaguar software.

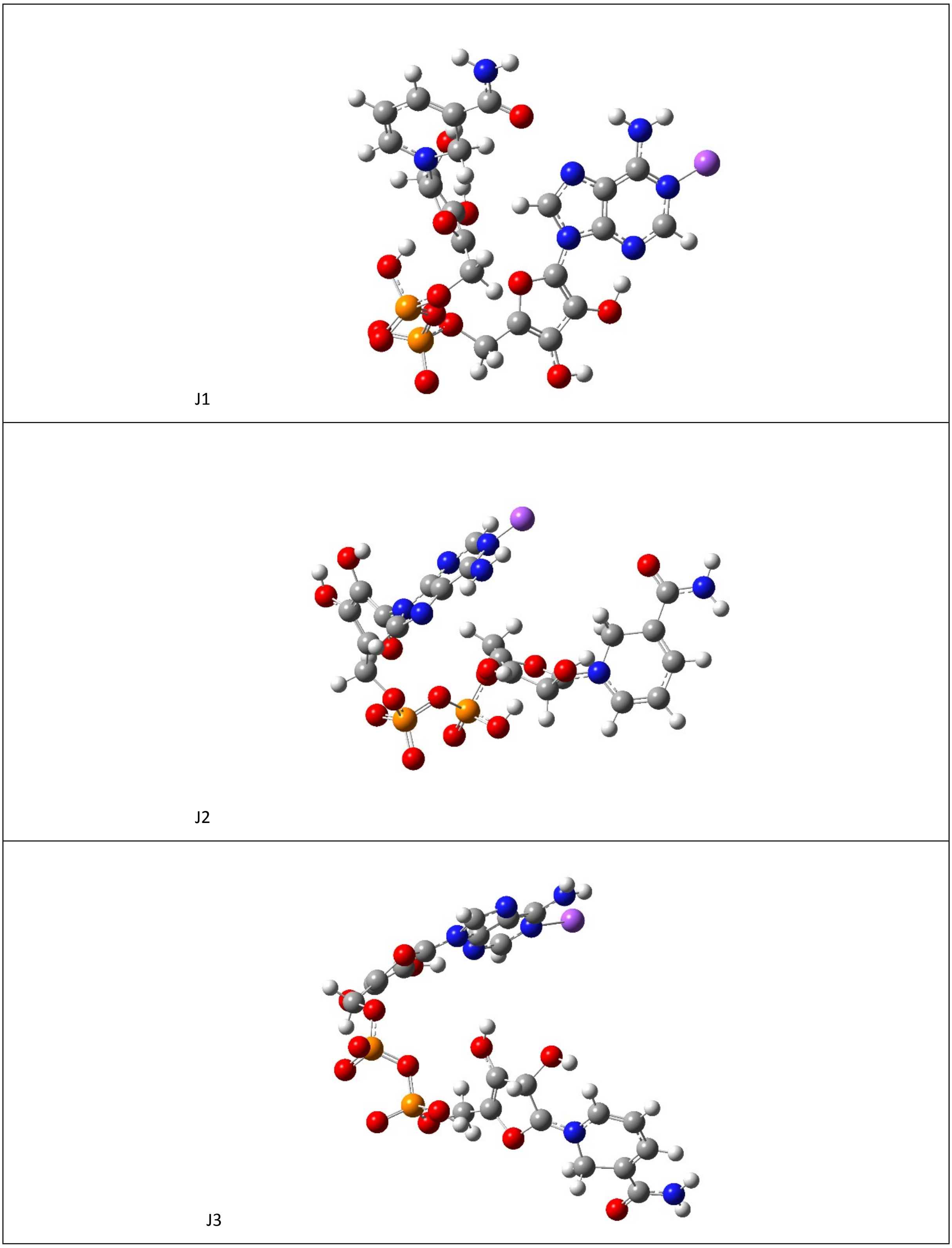

Figure S15. Lowest energy candidate structures proposed for the sodiated NAD^{+} IMS band J obtained at DFT/B3LYP/6-31G*using Jaguar software.

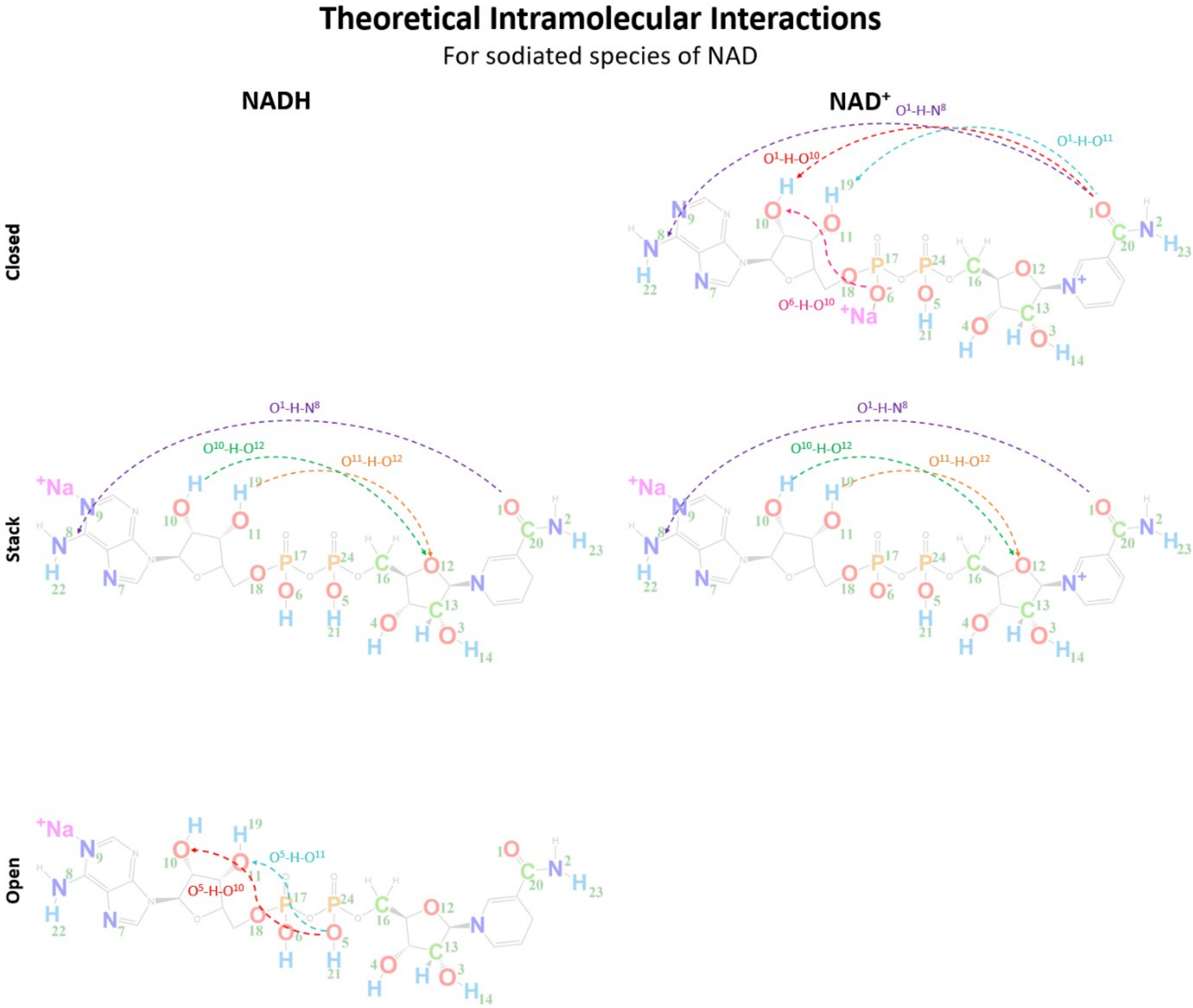

Figure S16. Intramolecular interactions of the sodiated species of NADH and NAD^+ sorted by the three main conformational families.

Table S1. Fluorescence decay parameters recovered for NADH in solution as a function of EtOH or MeOH content. NAD^+ is not fluorescent. The phase shift as a function the frequency was modeled using a double exponential model, where alpha (α) and tau (τ) are the pre-exponential factor and lifetime, respectively. The double exponential model was utilized assuming a two-state model: more "close" and more "open" conformations. The longer the lifetime, the more open the conformation.

	α_0	τ_0 (ns)	α_1	τ_1 (ns)	$\tau_{average}$ (ns)
10mM NH_4Ace pH 8.0	0.86	0.3	0.14	0.94	0.50
+10 % MeOH	0.86		0.14		0.52
+30 % MeOH	0.83		0.17		0.55
+50 % MeOH	0.81		0.19		0.57
+70 % MeOH	0.76		0.24		0.62
+10 % EtOH	0.83		0.17		0.55
+30 % EtOH	0.80		0.20		0.58
+50 % EtOH	0.73		0.27		0.64
+70 % EtOH	0.68		0.32		0.68

Table S2. Experimental and theoretical ion-neutral collision cross section (CCS_{N_2}, Å²) for the sodiated NAD⁺ and NADH forms.

				B3LYP/6-31G(d,p) with charges	
Ion		Group	Experimental CCS_{N_2} [Å²]	Theoretical CCS_{N_2} IMos TM [Å²]	Relative energy [kcal/mol]
$[M_{NADH} + Na]^+$ $C_{21}H_{30}N_7O_{14}P_2$ *m/z* 688.12 Δm/m 0.3 ppm	E_1	Stack	234	235.1	0
	E_2			235.8	10.27
	E_3			237.1	5.77
	F_1	Open	246	246.4	8.46
	F_2			245.8	6.39
	F_3			246.3	6.28
$[M_{NAD+} + Na]^+$ $C_{21}H_{28}N_7O_{14}P_2$ *m/z* 686.09 Δm/m 0.7 ppm	I_1	Close	227	229.5	0
	I_2			230.3	7.38
	I_3			228.6	7.19
	J_1	Stack	236	237.3	12.57
	J_2			237.8	1333
	J_3			237.5	12.58

Table S3. Experimental and theoretical ion-neutral collision cross section (CCS_{N_2}, Å^2) and experimental vibrational frequencies (cm^{-1}) for the protonated NADH form.

			B3LYP/6-31G(d,p) with charges		Experimental IR Bands and proposed interactions for $[M_{NADH} + H]^+$											
Ion		Exp. CCS [Å^2]	Theor. CCS IMos TM [Å^2]	Rel. energ [kcal/mol]	975 P-O(H) st.	1010 P-O(H) b.	1120 C-O(H) st.	1230 P-O(C)	1295 O-H b.	1340 P=O st.	3430 N-H-O st.	3450 NH_2 s st.	3540 O-H-O st.	3560 NH_2 a st.	3600 O-H st.	3660 (P)O-H st.
$[M_{NADH}+H]^+$ $C_{21}H_{30}N_7O_{14}P_2$ *m/z* 666.13 Δm/m 1.5 ppm	A	234	234.6	13.95	P^{24}-O^{5}	P^{24}-O^{5}-H^{21}	C^{13}-O^{3}-H^{14}		O^{11}-H^{19}			N^{2}/N^{8}	O^{5}-H^{21}-O^{11}	N^{2}/N^{8}	O^{3}-H^{14}	P^{24}-O^{5}-H^{21}
			234.3	14.37	P^{24}-O^{5}		C^{13}-O^{3}-H^{14}	P^{17}-O^{18}	O^{11}-H^{19}		N^{2}-H^{23}-O^{11}	N^{2}/N^{8}	O^{5}-H^{21}-O^{11}	N^{2}/N^{8}	O^{3}-H^{14}	P^{24}-O^{5}-H^{21}
			234.8	14.83	P^{24}-O^{6}	P^{24}-O^{5}-H^{21}	C^{13}-O^{3}-H^{14}		O^{11}-H^{19}	P^{17}-O^{6}		N^{2}/N^{8}	O^{5}-H^{21}-O^{11}	N^{2}/N^{8}	O^{3}-H^{14}	P^{24}-O^{5}-H^{21}
	B	239	239.4	0	P^{24}-O^{5}		C^{13}-O^{3}-H^{14}	P^{17}-O^{18}	O^{11}-H^{19}	P^{17}-O^{6}	N^{2}-H^{23}-O^{11}	N^{2}/N^{8}	O^{5}-H^{21}-O^{11}	N^{2}/N^{8}	O^{3}-H^{14}	P^{24}-O^{5}-H^{21}
			239.4	8.49		P^{24}-O^{5}-H^{21}	C^{13}-O^{3}-H^{14}		O^{11}-H^{19}	P^{17}-O^{6}		N^{2}/N^{8}	O^{5}-H^{21}-O^{11}	N^{2}/N^{8}	O^{3}-H^{14}	P^{24}-O^{5}-H^{21}
			239.2	4.67	P^{24}-O^{6}		C^{13}-O^{3}-H^{14}	P^{17}-O^{18}	O^{11}-H^{19}	P^{17}-O^{6}	N^{2}-H^{23}-O^{11}	N^{2}/N^{8}	O^{5}-H^{21}-O^{11}	N^{2}/N^{8}	O^{3}-H^{14}	P^{24}-O^{5}-H^{21}
	C	242	242.7	3.67	P^{24}-O^{5}	P^{24}-O^{5}-H^{21}	C^{13}-O^{3}-H^{14}	P^{17}-O^{18}	O^{11}-H^{19}	P^{17}-O^{6}	N^{2}-H^{23}-O^{11}	N^{2}/N^{8}	O^{5}-H^{21}-O^{11}	N^{2}/N^{8}	O^{3}-H^{14}	P^{24}-O^{5}-H^{21}
			242.1	11.73	P^{24}-O^{6}	P^{24}-O^{5}-H^{21}	C^{13}-O^{3}-H^{14}	P^{17}-O^{18}	O^{11}-H^{19}		N^{2}-H^{23}-O^{11}	N^{2}/N^{8}	O^{5}-H^{21}-O^{11}	N^{2}/N^{8}	O^{3}-H^{14}	P^{24}-O^{5}-H^{21}
			242.9	11.91	P^{24}-O^{5}	P^{24}-O^{5}-H^{21}	C^{13}-O^{3}-H^{14}	P^{17}-O^{18}	O^{11}-H^{19}	P^{17}-O^{6}	N^{2}-H^{23}-O^{11}	N^{2}/N^{8}	O^{5}-H^{21}-O^{11}	N^{2}/N^{8}	O^{3}-H^{14}	P^{24}-O^{5}-H^{21}

			244.2	7.29	P^{24}-O^{5}	P^{24}-O^{5}-H^{21}	C^{13}-O^{3}-H^{14}		O^{11}-H^{19}	P^{17}-O^{6}		N^{2}/N^{8}	O^{5}-H^{21}-O^{11}	N^{2}/N^{8}	O^{3}-H^{14}	P^{24}-O^{5}-H^{21}
	D	244	244.5	7.96	P^{24}-O^{5}		C^{13}-O^{3}-H^{14}	P^{17}-O^{18}	O^{11}-H^{19}		N^{2}-H^{23}-O^{11}	N^{2}/N^{8}	O^{5}-H^{21}-O^{11}	N^{2}/N^{8}	O^{3}-H^{14}	P^{24}-O^{5}-H^{21}
			244.5	9.10	P^{24}-O^{5}		C^{13}-O^{3}-H^{14}	P^{17}-O^{18}		P^{17}-O^{6}		N^{2}/N^{8}	O^{5}-H^{21}-O^{11}	N^{2}/N^{8}	O^{3}-H^{14}	P^{24}-O^{5}-H^{21}

Table S4. Experimental and theoretical ion-neutral collision cross section (CCS_{N_2}, $Å^2$) and experimental vibrational frequencies (cm^{-1}) for the protonated NAD^+ form.

			B3LYP/6-31G(d,p) with charges		Experimental IR Bands and proposed interactions for $[M_{NAD+} + H]^+$												
Ion		Exp. CCS [Å²]	Theor. CCS IMos TM [Å²]	Rel. energ [kcal/mol]	975 P-O(H) st.	1110 PO_2^- *s* st.	1115 C-O(H) st.	1190 P-O(C)	1240 O-H b.	1255 PO_2^- *as* st.	1340 P=O st.	1645 C=O st.	3430 N-H-O st.	3480 O-H-O st.	3540 O-H-O st.	3560 NH_2 a st.	3660 (P)O-H st.
$[M_{NAD+}+H]^+$ $C_{21}H_{28}N_7O_{14}P_2$ *m/z* 664.11 Δm/m 1.9 ppm	G	230	232.8	0	P^{24}-O^{5}	P^{24}	C^{13}-O^{3}-H^{14}		O^{3}-H^{14}	P^{17}		C^{20}-O^{1}	N^{2}-H^{23}-O^{11}	O^{3}-H^{14}-O^{6}	O^{5}-H^{21}-O^{11}	N^{2}/N^{8}	P^{24}-O^{5}-H^{21}
			232.6	7.05	P^{24}-O^{5}	P^{24}	C^{13}-O^{3}-H^{14}		O^{3}-H^{14}	P^{17}		C^{20}-O^{1}	N^{2}-H^{23}-O^{11}	O^{3}-H^{14}-O^{6}	O^{5}-H^{21}-O^{11}	N^{2}/N^{8}	P^{24}-O^{5}-H^{21}
			232.3	6.84	P^{24}-O^{5}	P^{24}	C^{13}-O^{3}-H^{14}		O^{3}-H^{14}	P^{17}		C^{20}-O^{1}		O^{3}-H^{14}-O^{6}	O^{5}-H^{21}-O^{11}	N^{2}/N^{8}	P^{24}-O^{5}-H^{21}
	H	246	246.8	5.84	P^{24}-O^{5}	P^{24}	C^{13}-O^{3}-H^{14}	P^{24}-O^{5}-C^{16}		P^{17}		C^{20}-O^{1}	N^{2}-H^{23}-O^{11}	O^{3}-H^{14}-O^{6}	O^{5}-H^{21}-O^{11}	N^{2}/N^{8}	P^{24}-O^{5}-H^{21}
			246.7	12.61	P^{24}-O^{5}	P^{24}	C^{13}-O^{3}-H^{14}		O^{3}-H^{14}	P^{17}		C^{20}-O^{1}	N^{2}-H^{23}-O^{11}	O^{3}-H^{14}-O^{6}	O^{5}-H^{21}-O^{11}	N^{2}/N^{8}	P^{24}-O^{5}-H^{21}
			246.0	7.48	P^{24}-O^{5}	P^{24}	C^{13}-O^{3}-H^{14}	P^{24}-O^{5}-C^{16}	O^{3}-H^{14}	P^{17}	P^{17}-O^{6}			O^{3}-H^{14}-O^{6}	O^{5}-H^{21}-O^{11}	N^{2}/N^{8}	P^{24}-O^{5}-H^{21}

Table S5. Theoretical intramolecular interactions of NADH.

					Vibrational Frequencies [cm^{-1}]								
					Characteristic of NADH					Present in Both			
Group		Exp. CCS_{N_2} [$Å^2$]	Theor. CCS_{N_2} [$Å^2$]	Rel. Energy [kcal/mol]	O^6-H-O^{10}	O^6-H-O^{11}	O^6-H-N^9	N^8-H-O^{12}	O^4-H-O^6	O^5-H-N^9	O^1-H-N^8	O^5-H-O^{11}	N^2-H-O^{11}
Close	A	234	234.6	13.95	3619		3287		3421		3349		
			234.3	14.37	3608		3280		3412		3339	3594	3409
			234.8	14.83	3615		3298		3419	3251			
Stack	B	239	239.4	0		3570	3288			3254	3303		3414
			239.4	8.49		3576	3282			3251	3306	3603	
			239.2	4.67		3568	3283			3250	3303	3593	3410
	C	242	242.7	3.67		3577		3443		3245	3310	3599	3428
			242.1	11.73		3579		3442		3249	3302		3425
			242.9	11.91		3583		3449		3251	3308	3597	3431
Open	D	244	244.2	7.29		3614			3425	3254	3309		
			244.5	7.96		3591			3417	3250	3301		3412
			244.5	9.10		3583			3411	3259	3312	3599	

Table S6. Theoretical intramolecular interactions of NAD^+.

					Vibrational Frequencies [cm^{-1}]								
					Characteristic of NAD^+					Present in Both			
Group		Exp. CCS_{N_2} [$Å^2$]	Theor. CCS_{N_2} [$Å^2$]	Rel. Energy [kcal/mol]	N^2-H-O^5	O^5-H-N^7	O^6-H-N^7	N^2-H-O^6	O^3-H-O^6	O^5-H-N^9	O^1-H-N^8	O^5-H-O^{11}	N^2-H-O^{11}
Close	G	230	232.8	0	3411		3227	3280	3463	3254	3314	3597	3423
			232.6	7.05	3417		3232	3279	3467	3250	3314	3601	3421
			232.3	6.84	3413		3229	3293	3468	3253	3322		
Open	H	246	246.8	5.84	3422	3617	3221		3468	3253			3412
			246.7	12.61	3416	3608	3219		3462	3247	3309	3602	3419
			246.0	7.48	3407	3614	3227		3455	3255		3595	